INTERNATIONAL JOURNAL FOR NUMERICAL AND ANALYTICAL METHODS IN GEOMECHANICS
Int. J. Numer. Anal. Meth. Geomech., 2000; **24**:281–303

Settlement-time behaviour of granular embankments

J. L. Justo*† and P. Durand

Department of Continuum Mechanics, University of Seville, E.T.S. Arquitectura, Avda. Reina Mercedes, 2, 41012 Sevilla, Spain

SUMMARY

Creep settlements are the main cause of deterioration of road pavement and impervious elements of dams, and therefore a method to calculate them is needed. Viscoelastic models (e.g. the standard linear solid) have been chosen to represent the creep of granular materials (Figure 1). Finite element calculations show that quasi-oedometric conditions exist near the centre of embankments. Explicit expressions for one-dimensional viscoelastic settlements of an embankment during and after construction have been obtained for any loading law and drawn for a linear load. The three viscoelastic parameters, E_o, R_c and T_r can be determined through laboratory or field testing, and the results can be adjusted by using settlement records. Good agreement has been found between measured and calculated settlements at several dams. Copyright © 2000 John Wiley & Sons, Ltd.

KEY WORDS: creep; viscoelasticity; granular materials; embankments; rockfill; finite elements

INTRODUCTION

Creep is a slow deformation of soil caused by constant effective stress. In rockfill dams and many earth dams, creep is responsible for the majority of post-constructive displacements which, in turn, may produce cracking of the impervious element or piping. Justo[1,2] has found positive correlations between the maximum crest settlement and the start of cracking or piping in embankment dams, and between this settlement and the amount of leakage in concrete face rockfill dams.[3] In 10–16 per cent of embankment dams with inadequate performance the cause was cracking or piping.[4]

Once the construction of the embankment has been completed, a dam should have sufficient camber at the top to allow postconstructive settlement without loss of freeboard. The importance of this point is supported by the fact that in 15 per cent of embankment dams with inadequate performance the cause was overtopping.[4] Due to this it is preferable to add an excess of camber during construction, as correction later on may be difficult and expensive. On the other hand, allowing for this excess might imply a great deal of extra cost.

In a road embankment post-constructive settlements may produce distortions in the grade, cracks on the road surface and steps between the road and structures.

* Correspondence to: Professor J. L. Justo, Department of Continuum Mechanics, University of Seville, E.T.S. Arquitectura, Avda. Reina Mercedes 2, 41012 Sevilla, Spain
† E-mail: Jarami@cica.es

Received 15 July 1998
Revised 4 November 1998; 7 April 1999

The need for a method to calculate creep in embankments is more than merely a matter of academic interest, as creep settlements of up to 1 m have been measured in some high modern embankments.[1,3]

Post-constructive settlements are not the only consequences of creep. In using elastic methods for building face dams, the modulus applied for water load is, on an average, 2·3 times greater[5,6] than it is during construction, which may be, at least partially, a result of creep. Finally, if creep is not included, calculated stresses produced by water load in the concrete face of dams may show opposite sign to what measured stresses indicate,[5,7] apart from other major discrepancies.[7] When creep is not taken into account there will be an underprediction of settlements even if elasto-plastic methods are utilized.[8]

Several authors have proposed linear relationships between creep strain and log of time in soils.[7,9–12] This semilogarithmic law implies that strain will tend to infinity when time tends to infinity. However, at least in some cases it seems that settlement finally ceases.[11,13–16] Results are also dependent on the uncertain time at which creep may start. In addition, for very high pressure (4–40 Mpa)[17] or in some rockfill dams (e.g. Wilmot dam)[12] the semilog law does not apply at all.

A FE method based upon the semilog law has shown good accordance with vertical settlement, but is not at all effective for predicting displacement and stresses in upstream face and downstream slope.[7]

In rockfill dams, as creep is activated by the rockfill's weight, several authors[5,18] have represented creep by a percentage of extra weight ranging from 16 to 36 per cent. Although there are no theoretical grounds for this method, the results obtained are valid. However, it is not possible to determine this percentage beforehand.

For all these reasons, checking if some viscoelastic rheological models fit the measured strains in rockfill could be illuminating. Extensive measurements of settlements in rockfill dams occurring under virtually one-dimensional conditions have shown that some of these models are effective in predicting settlement. For the sake of concision only a small part of these unpublished results will be included here.

2. THE APPLICATION OF RHEOLOGICAL MODELS TO CREEP ESTIMATE IN SOILS

2.1. Theory

Gibson and Lo[19] applied the standard linear solid rheological model of Figure 1 (a linear spring in series with a Kelvin model) to the study of clay consolidation and secondary compression. They claim that there is a good agreement with experimental results in normally consolidated clays. Christie[20] has shown that the results of this theory coincide with equations presented in 1939 by Merchant. Although the mechanism of creep is different, it would be interesting to verify if this model is applicable to granular materials.

The differential equation for this model (Figure 1) is

$$\sigma + T_r \frac{\partial \sigma}{\sigma t} = E_f \left(\varepsilon + T_r \frac{\partial \varepsilon}{\partial t} \right) \tag{1}$$

$$\text{where } E_o \text{ is the initial or elastic modulus, } E_f \text{ the final modulus} = (1/E_o + 1/E_1)^{-1} \tag{2}$$

$$\text{and } T_r \text{ the } \textit{relaxation time} = \eta/(E_o + E_1) = \eta(E_o - E_f)/E_o^2. \tag{3}$$

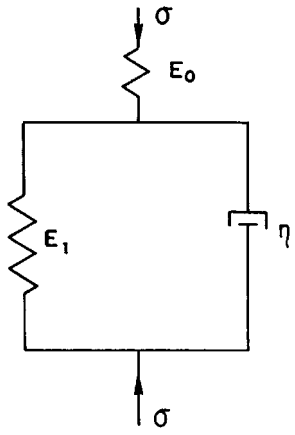

Figure 1. Standard linear solid

In a creep test ($\sigma = \sigma_o = \text{constant}$) the solution of equation (1) by integration will be

$$\varepsilon(T) = \frac{\sigma_o}{E_o}[R_c - (R_c - 1)e^{-T}] \tag{4}$$

$$\text{where } R_c = \frac{E_o}{E_f} = \textit{creep ratio} \text{ and} \tag{5}$$

$$T = t/T_r \text{ is called the } \textit{time factor}. \tag{6}$$

In a relaxation test ($\varepsilon = \varepsilon_o = \text{constant}$) the solution of equation (1) is

$$\sigma = E_o\varepsilon_o\left[\frac{1}{R_c} + \left(1 - \frac{1}{R_c}\right)e^{-T}\right] \tag{7}$$

The relaxation time is the time necessary to reach 63.2 per cent ($1 - e^{-1}$) of the total stress relaxation or the total creep strain.

Thompson[21] suggests using a spring in series with several Kelvin models to reproduce the linear relationship between strain and log time for extended periods. Zienkiewicz *et al.*[22] indicate that '*in practical problems seldom more than two Kelvin elements are needed to represent the material behaviour...*'.

The model of Figure 1 can suffer one-dimensional, isotropic or shear deformation. The corresponding moduli E would be the oedometric modulus, E_{oed}, the modulus of compressibility, K, or the rigidity modulus, G, respectively; the stresses σ the normal (σ) or shear stress (τ), and the strains ε the unit volume change (ε_v) or shear strain (γ). In this article a one-dimensional model is studied, leaving three-dimensional problems for a forthcoming paper.

If applied load varies with time according to Figure 2, the strain at time factor T will be given by the hereditary integral:

$$\varepsilon(T) = \int_0^T \frac{1}{E_o}[R_c - (R_c - 1)e^{-(T-T')}]\frac{d\sigma}{dT'}dT' \tag{8}$$

It is supposed that pressure maintains a constant value for $T \geqslant T_c$.

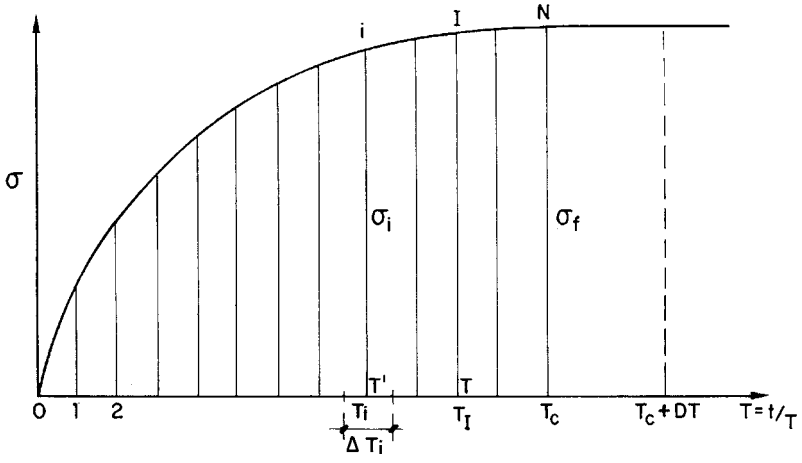

Figure 2. Load variable with time

The solution of the hereditary integral is

$$\varepsilon(T) = \frac{1}{E_o}[R_c\sigma - (R_c - 1)e^{-T}I_1] \tag{9}$$

where

$$I_1(\sigma, T) = \int_0^T e^{T'} \frac{d\sigma}{dT'} dT' \tag{10}$$

The strain in a process of loading from T up to T_c (Figure 2) will be

$$\Delta\varepsilon(T, T_c) = \varepsilon(T_c) - \varepsilon(T) \tag{11}$$

From equation (9):

$$\Delta\varepsilon(T, T_c) = \frac{1}{E_o}[R_c(\sigma_f - \sigma) - (R_c - 1)[e^{-T_c}I_1(\sigma, T_c) - e^{-T}I_1(\sigma, T)]] \tag{12}$$

For $T \geqslant T_c$, the strain from T_c up to $T_c + DT$ (Figure 2) will be

$$\Delta\varepsilon(T_c, T) = \varepsilon(T) - \varepsilon(T_c)$$

From equation (9):

$$\Delta\varepsilon(T_c, T) = \frac{R_c - 1}{E_o} I_1(\sigma, T_c) - e^{-T_c}(1 - e^{-DT}) \tag{13}$$

If the load varies linearly with time up to T_c, equation (13) becomes

$$\Delta\varepsilon(T_c, T) = \frac{\sigma_f(R_c - 1)}{E_o T_c}(1 - e^{-T_c})(1 - e^{-DT}) \tag{14}$$

If the loading curve does not correspond with a known function, it might be better to express the integral as a function of σ instead of $\partial\sigma/\partial T'$. Integrating I_1 by parts and substituting into (9):

$$\varepsilon(T) = \frac{1}{E_o}[\sigma + (R_c - 1)e^{-T} I_2] \tag{15}$$

where

$$I_2(\sigma, T) = \int_0^T \sigma e^{T'} \, dT'$$

The integral I_2 may be calculated using numerical methods:

$$I_2(\sigma, T) = \sum_{i=1}^{I} (\sigma_i e^{T_i} \Delta T_i) \tag{16}$$

where

$$\Delta T_i = \frac{T_{i+1} - T_{i-1}}{2}, \quad T_{I+1} = T_I \tag{17}$$

If the load varies linearly with time up to a maximum σ_f, then:

$$\text{For } T \leqslant T_c, \quad \frac{\varepsilon E_o}{\sigma} = R_c - (R_c - 1)\frac{1 - e^{-T}}{T} \tag{18}$$

$$\text{For } T \geqslant T_c, \quad \frac{\varepsilon E_o}{\sigma_f} = R_c - \frac{(R_c - 1)}{T_c}(e^{T_c} - 1)e^{-T} \tag{19}$$

Equation (18) is represented in Figure 3; the creep ratio R_c is the asymptotic value of $\varepsilon E_o/\sigma$ when $T \to \infty$, and is nearly reached for $T \geqslant 50$. Equations (18) and (19) are represented in Figure 4; the asymptotic value R_c is nearly reached for $T \geqslant 10$, when $T_c \leqslant 1$.

2.2. Application to an embankment

The height of the embankment increases with the time factor according to Figure 5. One-dimensional compression is assumed, and the stress at a point corresponds to the height of fill above it.

The settlement of a point at height z_I during construction will be (Figure 5):

$$s_c(z_I) = \int_0^{z_I} \Delta\varepsilon(T_I - T, T_c - T) \, dz \tag{20}$$

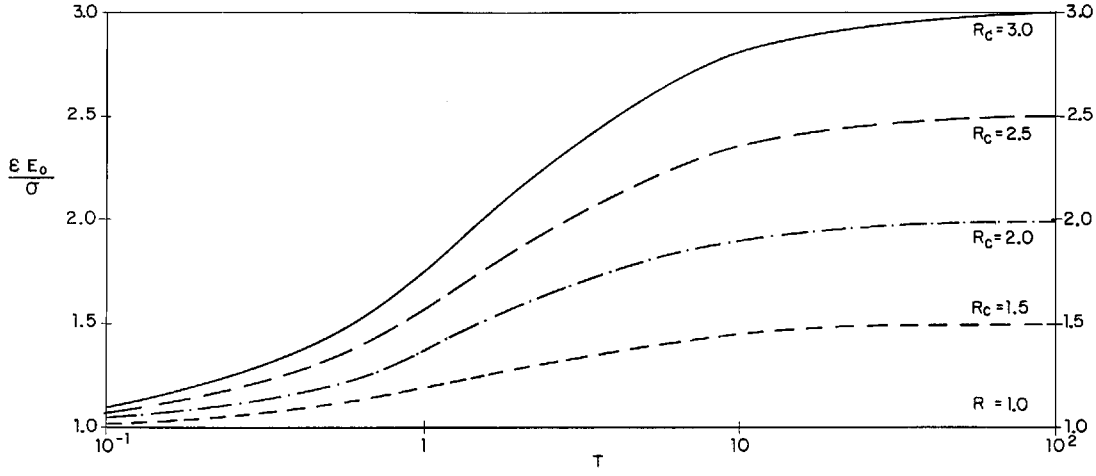

Figure 3. Strain during the linear application of load

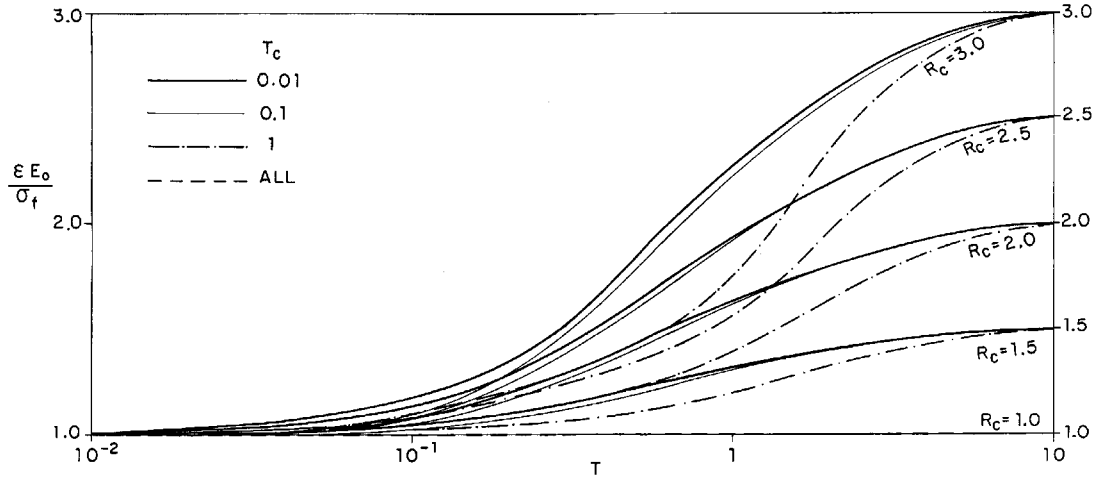

Figure 4. Strain during the linear application of load and when the load remains constant

$\Delta\varepsilon$ is obtained from equation (12):

$$\frac{\Delta\varepsilon E_o}{\gamma} = R_c Z_I - (R_c - 1)(e^{-T_c}[I_1(z, T_c) - I_1(z, T)] - e^{-T_I}[I_1(z, T_I) - (I_1(z, T)]) \qquad (21)$$

where

$$I_1(z, T) = \int_0^T e^{T'} \frac{dz}{dT'} dT' \qquad (22)$$

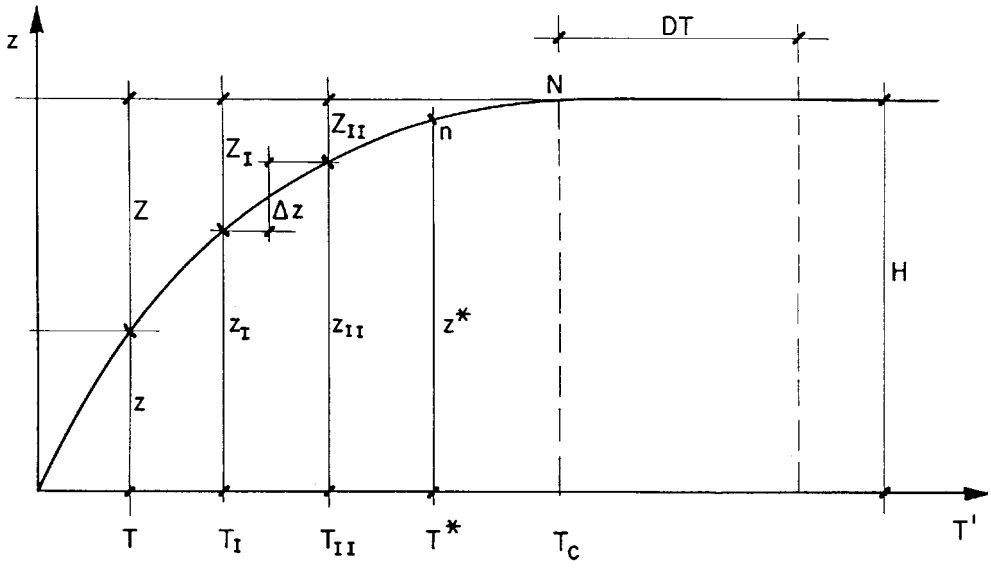

Figure 5. Height of embankment versus time factor

The integrals I that appear in this section and in Appendix I must be, in general, calculated by numerical methods. In order to do this the construction curve (Figure 5) is divided into I intervals from $T = 0$ up to T_I, and into $(N - I)$ intervals from $T = T_I$ up to $T = T_c$.

Substituting equation (21) into equation (20) and operating the settlement is finally obtained

$$\frac{s_c E_o}{\gamma} = R_c Z_I z_I - (R_c - 1)[b - e^{-T_I} I_3(z, T_I)] \tag{23}$$

where

$$b = e^{-T_c}[z_I I_1(T_I, T_c) + I_3(z, T_I)] \tag{24}$$

$$I_1(T_I, T_c) = \int_{T_I}^{T_c} e^T \frac{dz}{dT} dT = \sum_{i=I}^{N} (e^{T_i} \Delta z_i) \tag{25}$$

$$z_i = \frac{z_{I+1} - z_{I-1}}{2}, \quad z_{I-1} = z_I, \quad z_{N+1} = z_N \tag{26}$$

$$I_3(z, T_I) = \int_0^{T_1} z e^T \frac{dz}{dT} dT = \sum_{i=1}^{I} (z_i e^{T_i} \Delta z_i), \quad z_{I+1} = z_I \tag{27}$$

The relative heights are defined as

$$y = \frac{z}{H}, \quad Y = \frac{Z}{H} \tag{28}$$

Substituting into equation (23), the settlement can be put into non-dimensional form:

$$\frac{E_o s_c(y_I)}{\gamma H^2} = R_c Y_I y_I - (R_c - 1)[b' - e^{-T_I} I_3(z, T_I)] \tag{29}$$

where

$$b' = e^{-T_c}[y_I I_1'(T_I, T_c) + I_3'(y, T_I)] \tag{30}$$

$$I_1'(T_I, T_c) = \int_{T_1}^{T_c} e^T \frac{dy}{dT} dT = \sum_{i=I}^{N} (e^{T_i} \Delta y_i) \tag{31}$$

$$\Delta y_i = \frac{y_{i+I} - y_{i-1}}{2}, \quad y_{I-1} = y_I, \quad y_{N+1} = y_N \tag{32}$$

$$I_3'(y, T_I) = \int_0^{T_1} y e^T \frac{dy}{dT} dT = \sum_{i=1}^{I} (y_i e^{T_i} \Delta y_i), \quad y_{I+1} = y_I \tag{33}$$

The relative errors resulting from the numerical calculation of the integrals I included in this section and in Appendices I and II are $O(\Delta T^2)$.

If the height of the embankment varies linearly with time, then:

$$\frac{E_o s_c}{\gamma H^2} = R_c Y_I y_I - \frac{(R_c - 1)}{T_c^2}[1 + e^{-T_c} - e^{-T_c y_I} - e^{-T_c Y_I}] \tag{34}$$

Figure 6 shows non-dimensional settlement during construction (equation (34)) for different values of R_c and T_c. The following observations can be made:

1. For $R_c = 1$ the non-dimensional settlement is equal to

$$\frac{E_o s_c}{\gamma H^2} = Y_I y_I \tag{35}$$

2. The non-dimensional settlement greatly increases when T_c and R_c increase. When T_c tends to infinity:

$$\frac{E_o s_c}{\gamma H^2} = R_c Y_I y_I \tag{36}$$

3. The settlement is symmetrical with respect to the axis $y_I = 0{\cdot}5$.

The settlement of a point at height z_I after construction will be (Figure 5):

$$\Delta s(z_I) = \int_0^{z_I} \Delta \varepsilon(T_c, T_c + DT)\, dz \tag{37}$$

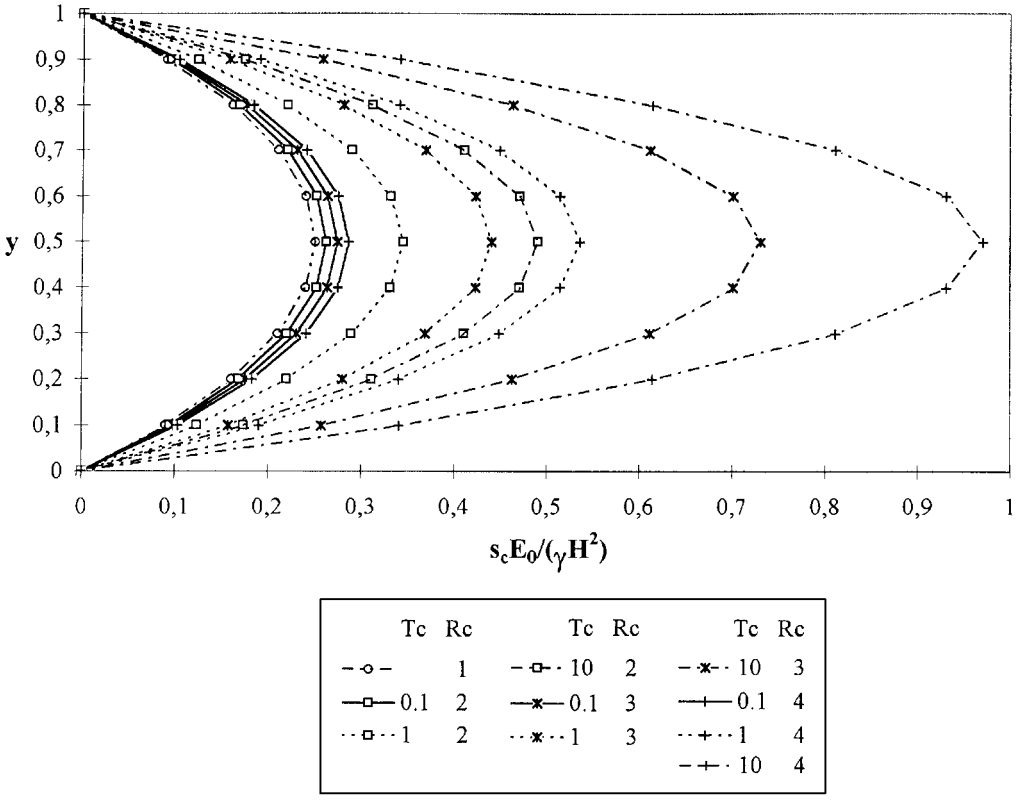

Figure 6. Non-dimensional settlement of an embankment during construction

Substituting the value of $\Delta\varepsilon$ into equation (13):

$$\frac{\Delta s E_o}{\gamma(R_c - 1)} = b(1 - e^{-DT}) \tag{38}$$

where b has the value of equation (24).
In non-dimensional form this settlement is

$$\frac{E_o \Delta s(y_I)}{\gamma H^2(R_c - 1)} = b'(1 - e^{-DT}) \tag{39}$$

where b' is determined by equation (30).
At the top of the embankment:

$$I'_1(T_c, T_c) = 0$$

$$\frac{E_o \Delta s(1)}{\gamma H^2(R_c - 1)} = e^{-T_c}(1 - e^{-DT}) I'_3(y, T_c) \tag{40}$$

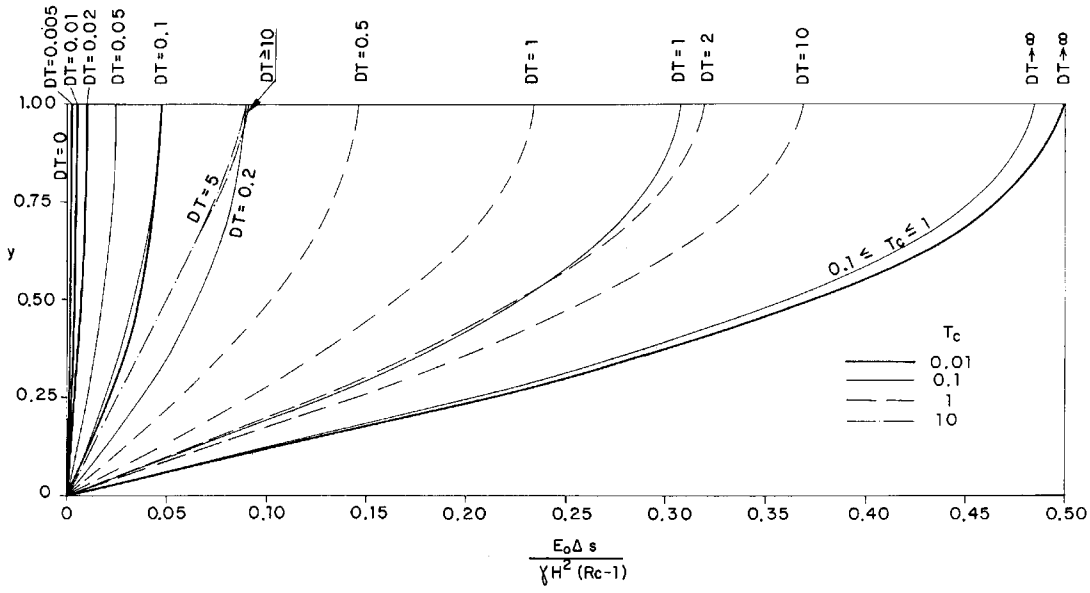

Figure 7. Non-dimensional settlement of an embankment after construction

If the height of the embankment varies linearly with time, then substituting equation (14) into (37), the non-dimensional settlement after the end of construction is

$$\frac{E_o \Delta s(z_I)}{\gamma H^2 (R_c - 1)} = \frac{1 - e^{-DT}}{T_c^2} (y_I T_c - e^{-T_c Y_I} + e^{-T_c}) \tag{41}$$

And at the top of the embankment:

$$\frac{E_o \Delta s(H)}{\gamma H^2 (R_c - 1)} = \frac{1 - e^{-DT}}{T_c} \left(1 - \frac{1 - e^{-T_c}}{T_c}\right) \tag{42}$$

Equation (41) is represented in Figure 7. For a given value of DT, the non-dimensional settlement increases when T_c decreases. When $T_c = 10$ there is a greater decrease of post-constructive settlement, as most of the settlement occurs during construction.

2.3. *Determining the parameters*

The three parameters that define the model are the initial or elastic modulus, E_o, the creep ratio, R_c, and the relaxation time T_r.

Charles[23] sustains that tests carried out with a large oedometer on rockfill samples 1 m in diameter and 0·5 m in height compacted to the same density and water content as that found in the embankment may be effective in predicting its constructional behaviour. He recommends utilizing an elastic calculation. Creep was not included in these calculations.

The three parameters may be obtained from oedometer tests in the way indicated below.

If the sample is subjected to a new process of loading, the initial conditions will be $\varepsilon = 0$ for $\sigma = 0$. Substituting into equation (1):

$$E_o = \frac{\partial \sigma}{\partial \varepsilon} \quad \text{for } t = 0 \tag{43}$$

So, the initial slope in the diagram of σ vs. ε will be the elastic modulus.

The ratio of creep strains at two different times t_2 and t_1 (for constant σ) will be obtained from equation (4):

$$\frac{\Delta\varepsilon(0, t_2)}{\Delta\varepsilon(0, t_1)} = \frac{1 - e^{-t_2/T_r}}{1 - e^{-t_1/T_r}} \tag{44}$$

The solution of this equation provides the relaxation time T_r.

Once E_o, and T_r have been found, the creep ratio, R_c, can be obtained from a creep test using equation (4):

$$R_c = \frac{E_o \varepsilon(T)/\sigma_o - e^{-T}}{1 - e^{-T}} \tag{45}$$

The laboratory determination of the parameters should only be used for preliminary calculations, as scale effects and differences in compaction might exist. In addition, creep deformations are dependent upon rainfall, which is difficult to reproduce in the laboratory, as it will be shown in the next section. For all these reasons the creep parameters should be corrected through monitoring of settlements during and after construction. It must be taken into account that a waiting period is sometimes specified before a road pavement is laid to ensure that later settlement will not damage the rolling surface. Settlement measurements taken during this period might be used to adjust the creep parameters.

If the settlements are measured at different heights inside the rockfill, then the 'strain' of a layer will permit the calculation of the creep parameters for that layer. The 'strain' of a finite layer during construction has been studied in Appendix I, and after construction in Appendix II. The ratio of strains after construction at any two different times is (see 66):

$$\frac{\Delta\varepsilon(T_c, T_2)}{\Delta\varepsilon(T_c, T_1)} = \frac{1 - e^{-DT_2}}{1 - e^{-DT_1}} = \frac{1 - e^{-\Delta t_2/T_r}}{1 - e^{-\Delta t_1/T_r}} \tag{46}$$

where Δt is the time increment after construction.

The solution of equation (46) will permit an adjustment for T_r.

Once T_r has been found, the creep ratio, R_c, can be obtained dividing the expressions of the 'strains' during construction (63) and after construction (66).

For $T^* = T_c$:

$$\frac{1}{R_c} = 1 - \frac{Z_{II}}{e^{-T_c}(I_1[T_{II}, T_c] + a)(1 + (1 - e^{-DT}/\Delta\varepsilon)\varepsilon_c) - a \times e^{-T_{II}}} \tag{47}$$

where the subindex c indicates the end of construction.

Once T_r and R_c have been found, equation (63) is used to calculate E_o. For $T^* = T_c$:

$$E_o = \frac{\gamma}{\varepsilon_c}(R_c Z_{II} - (R_c - 1)[e^{-T_c} I_1(T_{II}, T_c) + a(e^{-T_c} - e^{-T_{II}})]) \tag{48}$$

If the settlements are measured at only one height (e.g. at surface), the average creep parameters for the embankment can only be obtained up to that height. Relaxation time may be determined using the ratio of equation (38) for two different times:

$$\frac{\Delta s(z_I, T_2)}{\Delta s(z_I, T_1)} = \frac{1 - e^{-\Delta t_2/T_r}}{1 - e^{-\Delta t_1/T_r}} \tag{49}$$

From equations (23) and (38):

$$\frac{1}{R_c} = 1 - \frac{Z_I z_I}{b(1 + (1 - e^{-DT}/\Delta s)s_c) - e^{T_I} I_3(z, I_I)} \tag{50}$$

From equation (23):

$$E_o = \frac{\gamma}{s_c}(R_c Z_I z_I - (R_c - 1)[b - e^{-T_1} I_3(z, T_I)]) \tag{51}$$

3. EXPERIMENTAL VERIFICATION

Martin Gonzalo is an upstream facing rockfill dam,[24] that suffered a rupture in its membrane during filling of the reservoir. Six batteries of settlement plates (*A* to *F*) were placed (Figure 8) and measurements made during construction and up to six years after the completion of the construction.

Holz and Hilf[15] described the *collapse* of a soil's structure when wetted, and employed this term to label the resulting settlement. Many authors have utilized the same term referring to both cohesive and granular materials,[7,13,14,25–27] although other terms such as *hydrocompaction* have also been employed. According to Terzaghi[28] *collapse* in granular materials is related to the decrease in the particles' crushing strength, specially at the contact points.[10] Collapse is time dependent.[28,29]

Figure 9 shows the strain of different layers for settlement plates set *C* for times after fill placement. Accumulated rainfall is drawn in the same graph, showing a clear correlation between the creep and rainfall rates, due to the collapse settlement during the first 800 days after construction. Later on, when rockfill reaches a maximum wetting point and the rearrangement of rocks has occurred, rainfall does not produce more settlements.[30] It is not possible at present to relate collapse within a mass of rockfill with the rate of rainfall, so we have included it within the creep settlement. In this way, calculated creep could simulate the average trend, although not the sharp steps of collapse settlement's true strain.

So as to evaluate the strain of rockfill in a simple way, it has been assumed that in the central part of the dam there are only vertical displacements, and the vertical stress corresponds to overburden pressure. In this way, the vertical strain will be

$$\varepsilon_z = \frac{\gamma Z}{E_{oed}} \tag{52}$$

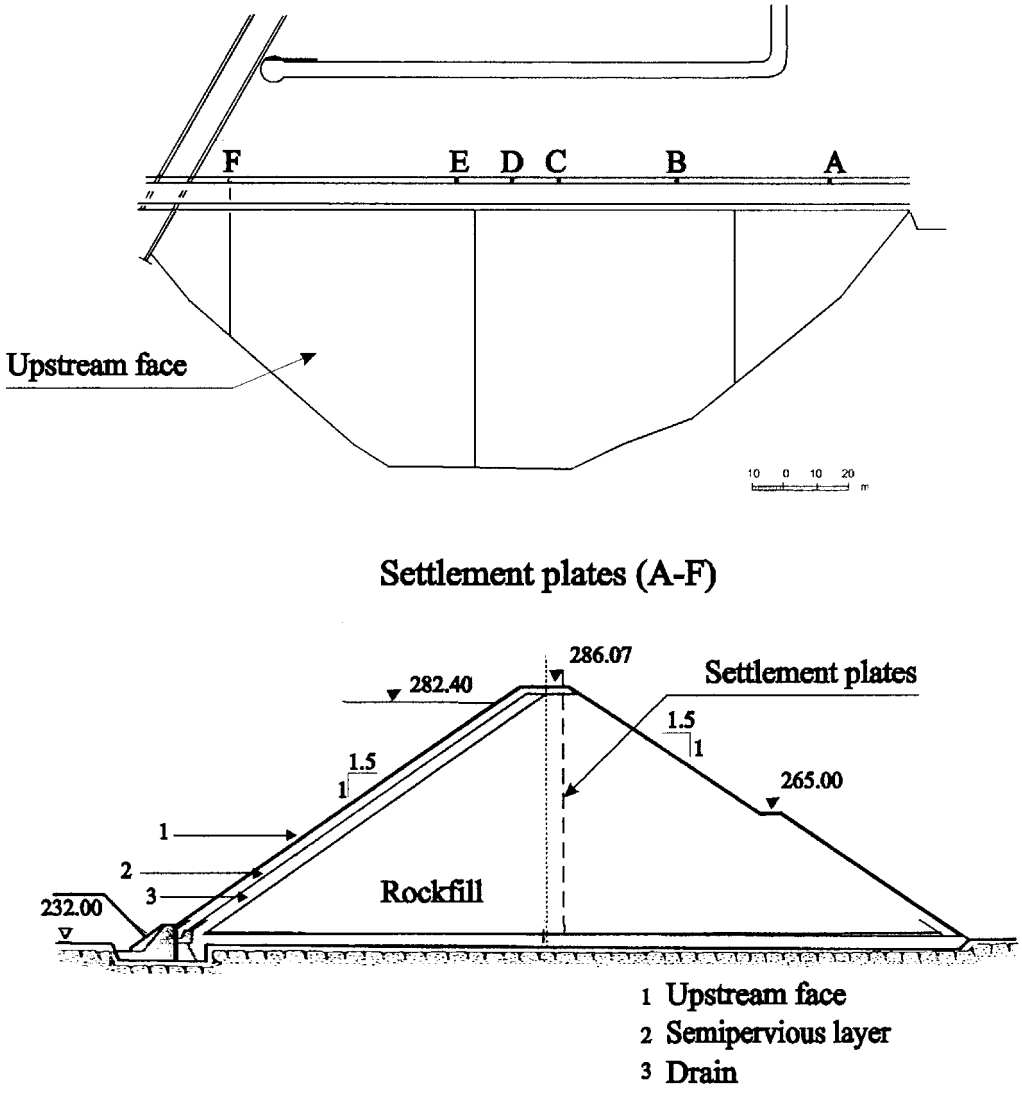

Figure 8. Martin Gonzalo rockfill dam. Lay-out of settlement plates

It has been proven in Martin Gonzalo Dam that the vertical strain calculated by equation (52) is similar to the vertical strain obtained from a three-dimensional finite element calculation (Figure 10). This is a consequence of quasi-oedometric conditions existing near the centre of the dam.

The T_r, R_c and E_o parameters for every layer have been found from field records, as indicated in Section 2.3. The presence of collapse after heavy rainfall produces differences in the T_r and R_c

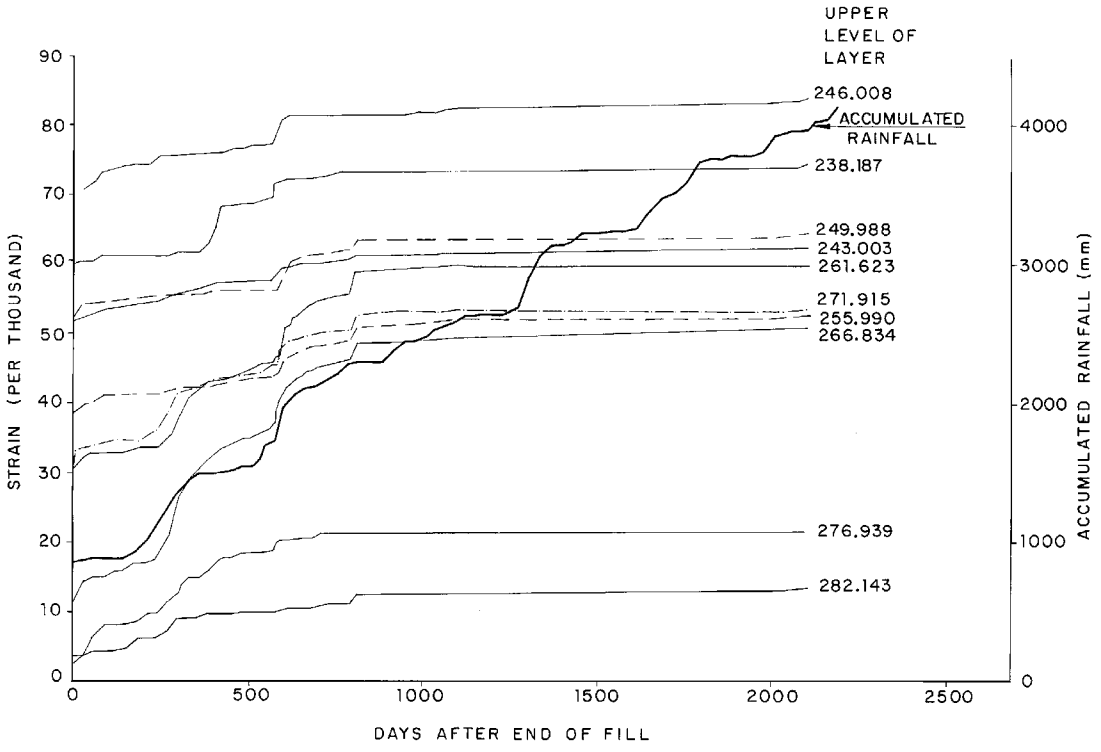

Figure 9. Strain of the different layers at settlement plates set *C*, and rainfall after filling

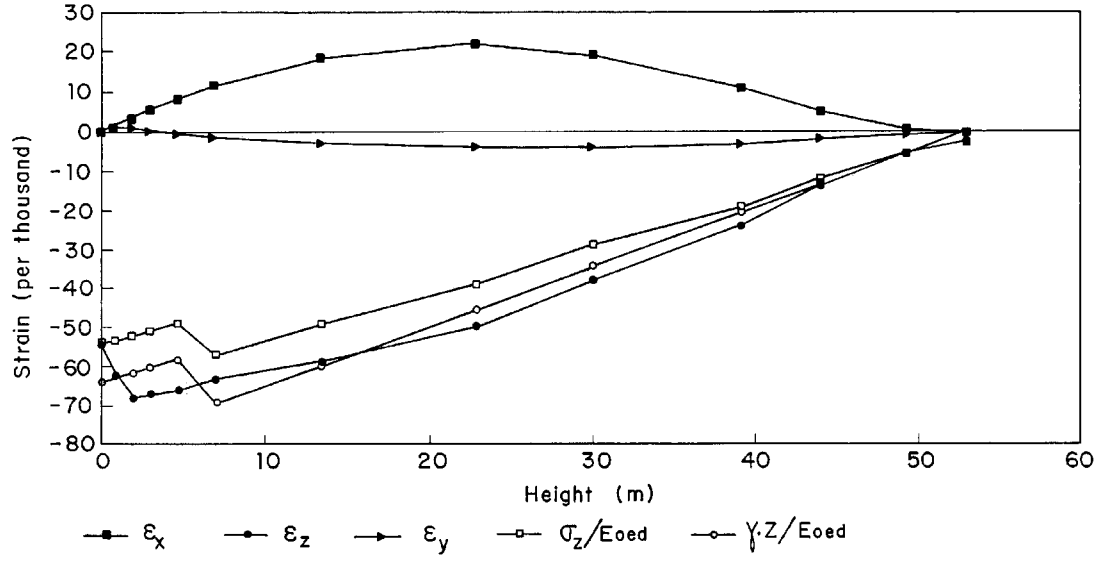

Figure 10. Strains in plate set *C*. Comparison between ε_z and σ_z/E_{oed} obtained by FE method, and $\gamma Z/E_{oed}$

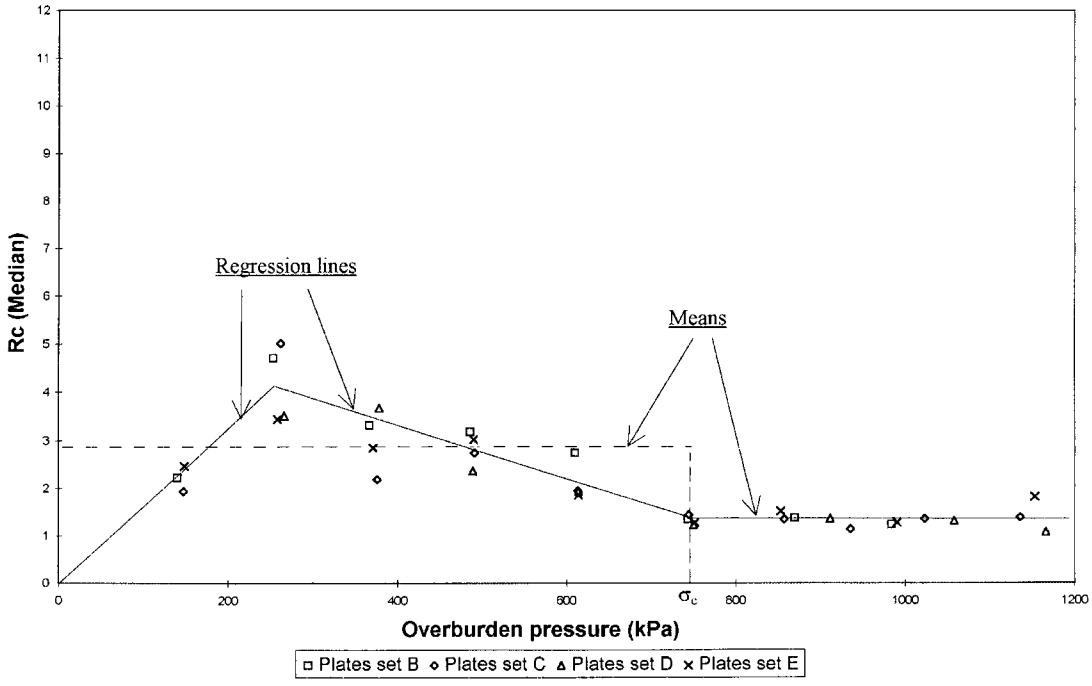

Figure 11. Creep ratio as a function of average stress in different layers

values obtained at different times after the construction. There is also scattering of the three parameters from layer to layer due to the variability of rockfill. However there is no clear trend in the variation of either T_r or R_c with respect to time, therefore median values have been taken.

The variation of T_r with respect to pressure is complex, but the median value has also been selected for each set of plates. On the other hand, E_o is constant during most of the pressure range (except for very low-pressure values) indicating linear elastic behaviour, and again the median value for each set of plates has been selected.

R_c is stress dependent (Figure 11), and the variation of the creep ratio with respect to pressure is quite similar to the variation of collapse:[29,30] the creep ratio increases with stress level up to a maximum and then decreases to a constant low value (in the case of collapse this constant is zero). The corresponding regression lines and the standard error about regression are indicated in Table I. Scattering for $\sigma < 745$ kPa is quite great owing to the variability of rockfill's different layers with pieces up to 600 mm. On the other hand, for $\sigma \geqslant 745$ kPa, R_c has a rather low coefficient of variation (12 per cent) and is almost constant ($\overline{R_{c2}} = 1{\cdot}34$). Owing to the large amount of scattering for $\sigma < 745$ kPa the mean value of R_c ($\overline{R_{c1}} = 2{\cdot}88$) has been selected for calculation. A test of significance has been carried out to see if the difference between the two means may be due to scattering. The probability that ($\overline{R_{c1}} - \overline{R_{c2}}$) may be less than zero is negligible (3×10^{-7}), so the difference between both values is extremely significant. Therefore, in the calculations a discontinuity in the R_c values has been assumed. This discontinuity appears only in soft rockfills; when a certain pressure, σ_c, is reached in these, the grains attain stable

Table I. Frequency distribution and regression equations for the creep ratio R_c

σ (kPa)	Regression line	Standard error about the regression (s)
<255	$R_c = 0{\cdot}01587\sigma$	0·39
255–745	$R_c = 5{\cdot}38 - 0{\cdot}00542\sigma$	0·51
$\geqslant 745$	$\overline{R_{c2}} = 1{\cdot}34$	0·17
<745	$\overline{R_{c1}} = 2{\cdot}88$	0·90

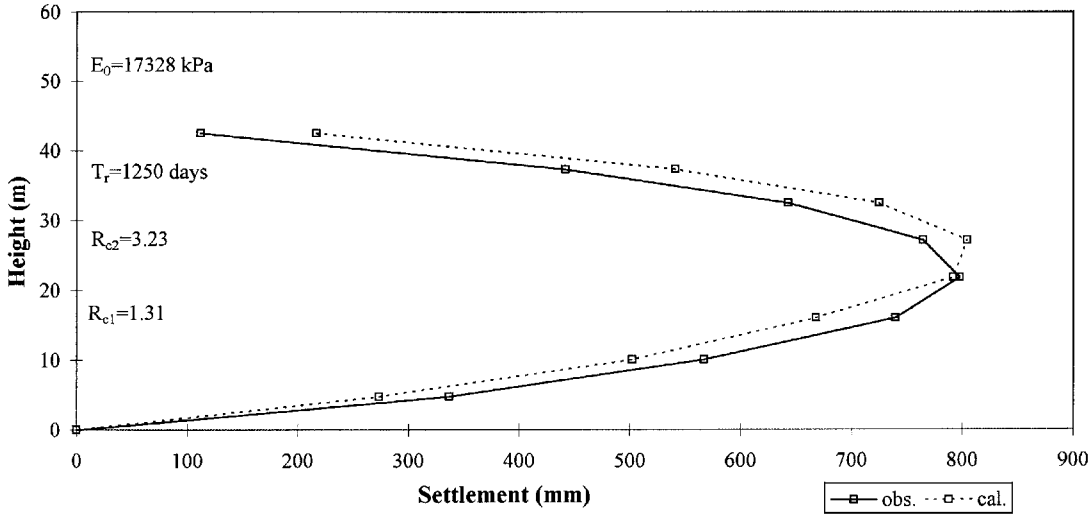

Figure 12. Comparison between observed and calculated settlements at the end of construction. Plates set *B*

positions and the subsequent slides are minor. As it will be now shown, it has been verified that using median values of T_r and E_o for each set of plates and only a two-step variation of R_c, an acceptable estimate of the settlement at different levels during and after construction may be obtained.

The settlement of a two-layer embankment (with different values of R_c) has been studied in Appendices I (during construction) and II (after construction).

The median value of the oedometric modulus E_o for the whole dam is 17,109 kPa. With $\nu = 0{\cdot}29$ (obtained from Jaky's equation for the angle of internal friction) it corresponds to a modulus of elasticity of 13,056 kPa. The average modulus obtained during construction in 60 cm diameter plate loading tests was 13,240 kPa, very close to the value obtained from settlement records interpreted according to the viscoelastic theory.

Figure 12 shows measured and calculated settlements at the end of construction obtained by equations (23) and (53) at plates set B. Figure 13 shows measured and calculated settlements at different plates (set B) after construction obtained with equations (38) and (67). The agreement of

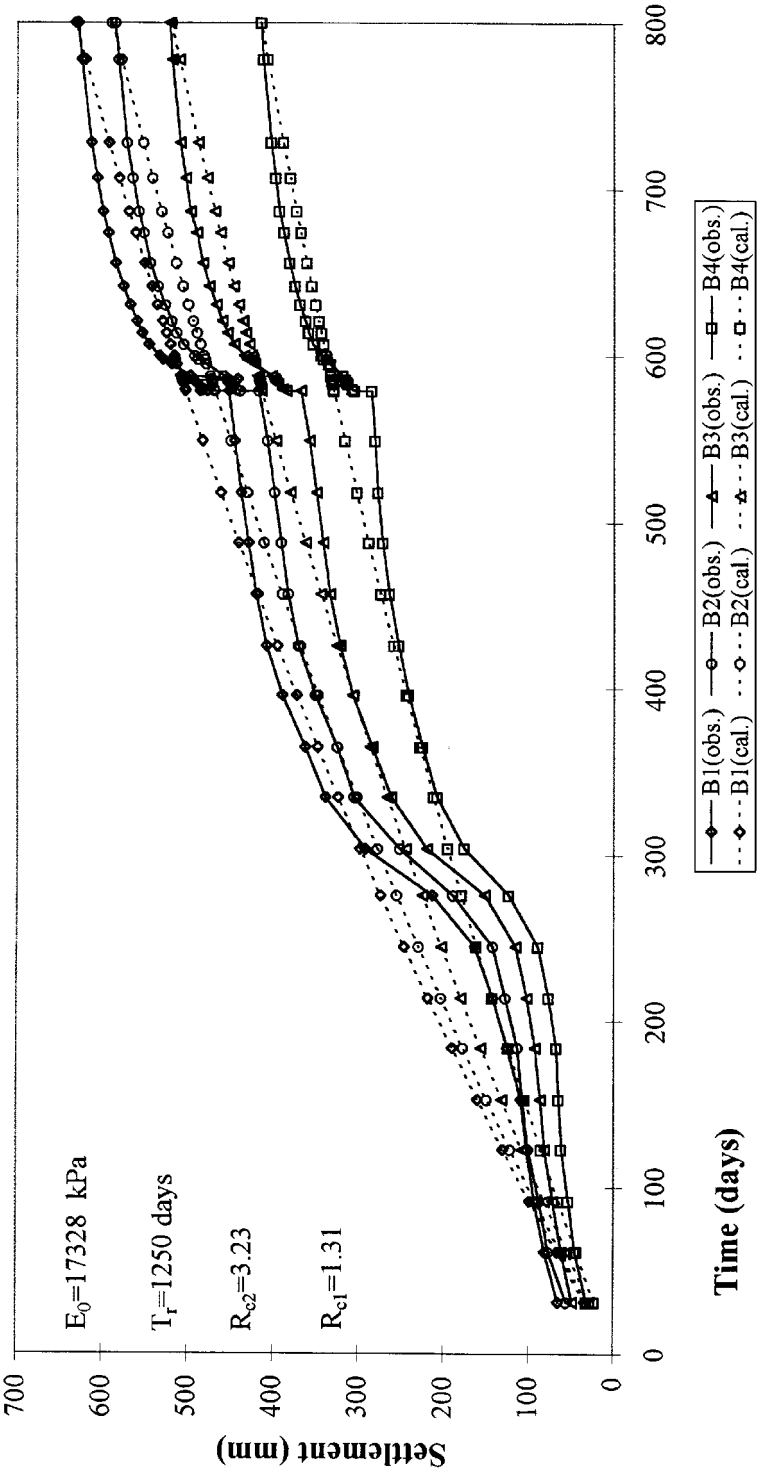

Figure 13. (a) Comparison between observed and calculated settlements after construction. Plates 1 (upper) to 4 (set *B*).

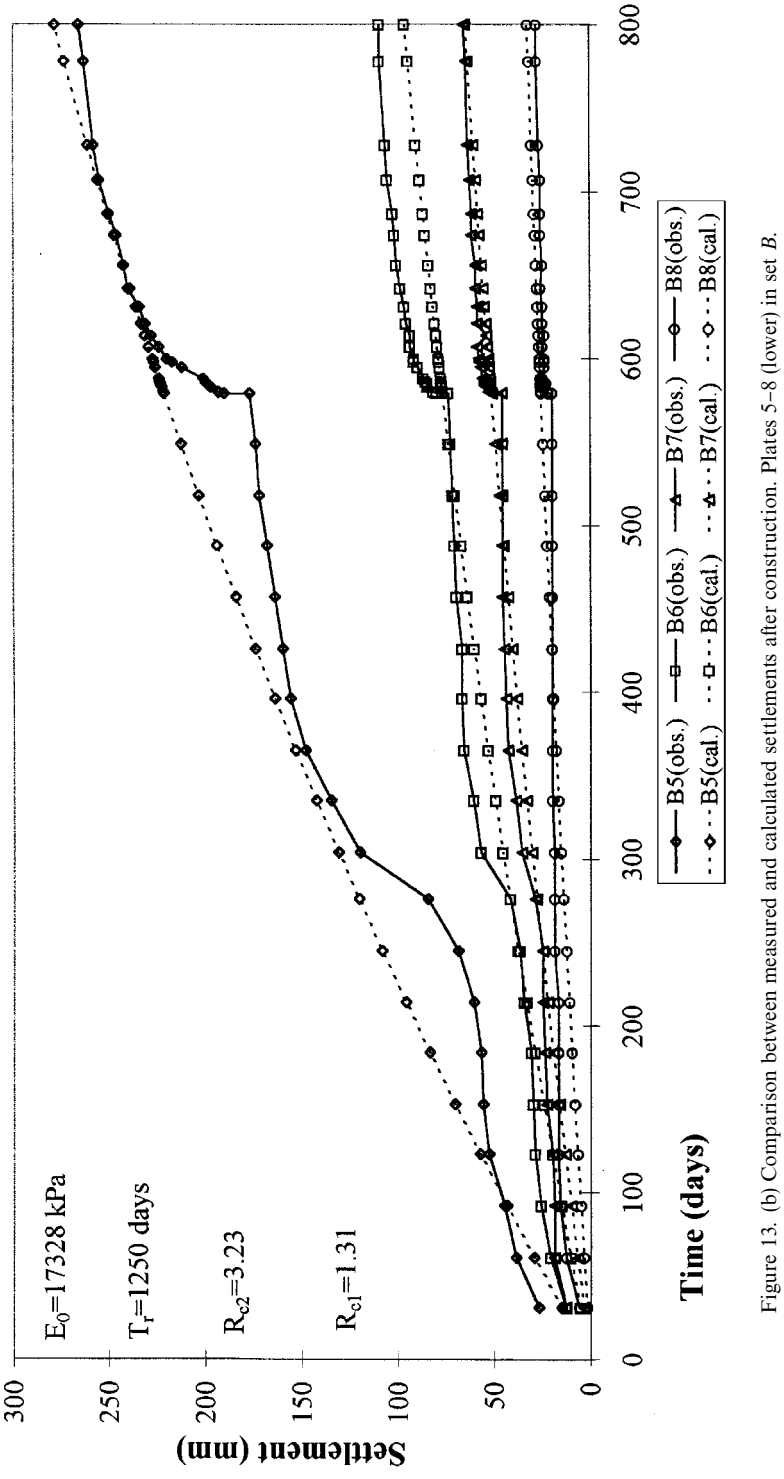

Figure 13. (b) Comparison between measured and calculated settlements after construction. Plates 5–8 (lower) in set *B*.

Table II. Creep parameters R_c and T_r at several dams[27]

Material	Dam	T_r (days)	σ (kPa)	R_c
Rockfill	Beliche (Portugal)		All	1·28
	Martin Gonzalo (Spain)	800	$<\sigma_c$	2·88
	Martin Gonzalo (Spain)	800	$>\sigma_c$	1·34
Transition	Beliche (Portugal)	1667	All	1·20
	Canales (Spain)	833	All	1·35
	Yeguas (Spain)	143	<700	1·55
	Yeguas (Spain)	143	>700	1·07
Core	Canales (Spain)		All	1·44
	Beliche (Portugal)	1064	All	1·15
	Yeguas (Spain)	125	<700	1·30
	Yeguas (Spain)	125	>700	1·07

σ_c ranges from 600 to 750 kPa

the results is excellent, although the measured settlement is more irregular due to rainfall-induced collapse.

This agreement for each layer of the dam, using single values of the parameters for the whole plates set, suggests that the viscoelastic model is consistent with the one-dimensional compression of coarse granular materials. The same result has been obtained in other plates sets and other dams (see Table II).

Table II shows the average values of the creep ratio and relaxation time calculated from several materials and dams. The creep ratio may range from a little more than 1 to 2·88 (in some rockfills). The relaxation time ranges from 125 days (quick creep) in core material to 1667 days (slow creep) in soft rockfill. The step for the creep ratio existing in the Martin Gonzalo rockfill and Yeguas transition does not exist in other similar materials.

4. CONCLUSIONS

The use of viscoelastic rheological models (e.g. the standard linear solid) to quantify the creep of granular materials is presented in this paper. Figure 10 demonstrates that quasi-oedometric conditions of deformation exist near the centre of embankments. This article has been restricted to one-dimensional calculations, where viscoplastic models are not applicable. The three-dimensional case has been left for a forthcoming paper. Under these circumstances three parameters define the model: the elastic modulus, E_o, related with the elastic strain, the creep ratio, R_c (ratio of total to elastic strains under constant stress) and the relaxation time, T_r, which controls the strain rate. For three-dimensional calculations only Poisson's ratio needs to be added.

Explicit expressions for one-dimensional settlements and strains of an embankment during and after construction have been found for any loading law and drawn for a linear increase of the height of the embankment.

It has been explained how to determine the three viscoelastic parameters through laboratory tests, and how to correct them with field settlement measurements during and after construction.

In an embankment, collapse produced by rainfall interacts with creep and causes irregularities in settlement. A unique set of settlement records that allows creep study has been collected in

Martin Gonzalo dam during construction and up to six years after the completion of the construction. Good agreement has been found between the measured and calculated settlements at Martin Gonzalo and several other dams constructed with granular materials, using median values of T_r and E_o.

The variation of the creep ratio in soft rockfill with respect to pressure is similar to the pressure dependence of collapse (Figure 11). Notwithstanding, for calculations, a threshold for stresses between 600 and 750 kPa may be assumed: R_c suffers a strong decrease when this threshold is surpassed.

The proposed method allows calculation of the wait-time needed before paving a road embankment so that the remaining settlement is allowable. This is not possible with the empirical semilog procedure in which the remnant settlement is always infinite. The method presented is based upon three parameters with a clear physical meaning. The range of the creep parameters R_c and T_r has been established in Section 3 following detailed study of creep deformations in several dams.

Empirical correlations between the maximum crest settlement and the cracking of face dams also permit the calculation of wait-time before the face is constructed.

The model may be extended to other materials, such as ideal crosslinked polymers. In the future several Kelvin models in series with a spring will be tried to improve the estimate of the complex behaviour of rockfill and other materials.[22]

APPENDIX I

I.1. One-dimensional settlement of a point in a two-layer embankment

If the embankment has a creep R_{c1} up to height h (reached at a time factor T_h) and R_{c2} in the remainder, the non-dimensional settlement at the end of construction is calculated in the following way:

For $z_I < h$ by equation (23) with $R_c = R_{c1}$

For $z_I > h$ by the following equation:

$$\frac{s_c E_o}{\gamma} = Z_I[h(R_{c1} - R_{c2}) + R_{c2} z_I] + h[e^{-T_c} I_1(T_h, T_c) - e^{-T_I} I_1(T_h, T_I)](R_{c2} - R_{c1}) - (e^{-T_c} - e^{-T_I})[(R_{c1} - 1) I_3(z, T_h) + (R_{c2} - 1) I_3(T_h, T_I)] - (R_{c2} - 1) z_I e^{-T_c} I_1(T_I, T_c) \tag{53}$$

where $I_1(T_h, T_c)$ and $I_1(T_h, T_I)$ are obtained with equations similar to (25), $I_3(z, T_h)$ with an equation equivalent to (27), and:

$$I_3(T_h, T_I) = \int_{T_h}^{T_I} z e^T \frac{dz}{dT} dT = \sum_{i=I_h}^{I} (z_i e^{T_i} \Delta z_i) \tag{54}$$

where I_h is the number of intervals up to T_h in the curve of Figure 5.

I.2. 'Strain' of a finite layer during construction

The 'strain' of a layer during construction may be measured from the settlements of two plates placed at bottom (I) and top (II) of the layer (Figure 5). The compression of the layer can only be determined from the time once the upper plate is placed:

The strain from time factor T_{II} up to T^* is

$$\Delta\varepsilon = \Delta\varepsilon(T_{II} - T, T^* - T) \tag{55}$$

Substituting T_I by T_{II} and T_c by T^* into equation (21):

$$\frac{\Delta\varepsilon E_o}{\gamma} = R_c(z^* - z_{II}) - (R_c - 1)[e^{-T^*} I_1(z, T^*) - e^{-T_{II}} I_1(z, T_{II}) + (e^{-T_{II}} - e^{-T^*}) I_1(z, T)] \tag{56}$$

The compression of the layer is

$$\Delta s(z_I, z_{II}) = \int_{z_I}^{z_{II}} \Delta\varepsilon \, dz \tag{57}$$

Operating:

$$\frac{\Delta s E_o}{\gamma} = R_c(z^* - z_{II})\Delta z - (R_c - 1)[e^{-T^*} \Delta z I_1(T_{II}, T^*) + a\Delta z(e^{-T^*} - e^{-T_{II}})] \tag{58}$$

where

$$a = \frac{I_3(T_I, T_{II}) - z_I I_1(T_I, T_{II})}{\Delta z} \tag{59}$$

$$I_3(T_I, T_{II}) = \int_{T_I}^{T_{II}} z e^T \frac{dz}{dT} \, dT = \sum_{i=I}^{i=II} (z_i e^{T_i} \Delta z_i) \tag{60}$$

$$I_1(T_I, T_{II}) = \int_{T_I}^{T_{II}} e^T \frac{dz}{dT} \, dT = \sum_{i=I}^{i=II} (e^{T_i} \Delta z_i) \tag{61}$$

$$\Delta z_i = \frac{z_{i+1} - z_{i-1}}{2}, \quad z_{I-1} = z_I, \quad z_{II+1} = z_{II} \tag{62}$$

The 'strain' of a finite layer during construction is defined as

$$\varepsilon = \varepsilon(z_I, z_{II}) = \frac{\Delta s}{\Delta z}$$

$$\frac{\varepsilon E_o}{\gamma} = R_c(z^* - z_{II}) - (R_c - 1)[e^{-T^*} I_1(T_{II}, T^*) + a(e^{-T^*} - e^{-T^{II}})] \tag{63}$$

$$I_1(T_{II}, T^*) = \int_{T_{II}}^{T^*} e^T \frac{dz}{dT} \, dT = \sum_{i=II}^{N} (e^{T_i} \Delta z_i), \quad z_{II-1} = z_{II} \tag{64}$$

APPENDIX II

II.1. 'Strain' of a finite layer after the end of construction

The 'strain' of a finite layer (z_I to z_{II} in Figure 5) after construction will be

$$\Delta\varepsilon = \frac{\Delta s(z_I, z_{II})}{\Delta z} = \frac{\Delta s(z_{II}) - \Delta s(z_I)}{\Delta z} \tag{65}$$

$$\frac{\Delta\varepsilon E_o}{\gamma(R_c - 1)} = e^{-T_c}(1 - e^{-DT})[I_1(T_{II}, T_c) + a] \tag{66}$$

where a is obtained from equation (59) and $I_1(T_{II}, T_c)$ from equation (61), exchanging T_I by T_{II} and T_{II} by T_c.

II.2. Settlement of a two-layer embankment after the end of construction

For a two-layer embankment with creep ratios R_{c1} and R_{c2} in the lower and upper layers, respectively, the settlement after construction is

For $z_I > h$:

$$\frac{E_o \Delta s(z_I)}{\gamma} = e^{-T_c}(1 - e^{-DT})([R_{c1} - R_{c2}][hI_1(T_h, T_c) + I_3(z, T_h)] + (R_{c2} - 1)(z_I I_1(T_I, T_c) + I_3(z, T_I))) \tag{67}$$

where the integrals I_1 and I_3 have the values indicated in Appendix I or in Section 2.2.

For $z_I < h$ the settlement is obtained by equation (41) with $R_c = R_{c1}$.

REFERENCES

1. J. L. Justo, 'The cracking of earth and rockfill dams', *Trans 11th Int. Cong. on Large Dams*, Vol. 4, Madrid, 1973, pp. 921–945.
2. H. H. Thomas, *The Engineering of Large Dams*, Part 2, Wiley, London, 1979, pp. 409–410.
3. J. L. Justo and A. González, 'Las presas de escollera con pantalla de hormigón armado', *Rev. Obras Públicas*, Madrid, March, 1986, pp. 173–194.
4. U.S. Committee on Large Dams, *Lessons from Dam Incidents*, ASCE, NY 1975.
5. J. L. Justo,m F. Segovia and A. Jaramillo, 'Three-dimensional joint elements applied to concrete-faced dams', *Int. J. Numer. Anal. Meth. Geomech.*, **19,** 615–636 (1995).
6. P. L. Marques, E. Maurer and N. B. Toniatti, 'Deformation characteristics of Foz do Areia concrete face rockfill dam, as revealed by a simple instrumentation system', *Trans. 15th Int. Cong. on Large Dams*, Vol. 1, Lausanne, 1985, pp. 417–450.
7. Central Board of Irrigation and Power, *Rockfill Dams*, Balkema, Rotterdam (1992).
8. J. L. Justo, 'Design parameters for special soil conditions'. General Report. *Proc. 7th European Conf. Soil Mech. & F.E.*, Vol. 5, 1979, pp. 127–158.
9. K. Buisman, 'Results of long duration settlement tests', *Proc. 1st Int. Conf. Soil Mech. & F.E.*, Vol. 1, pp. 103–106, 1936.
10. G. F. Sowers, R. C. Williams and T. S. Wallace, 'Compressibility of broken rock and the settlement of rockfills', *Proc. 6th Int. Conf. Soil Mech.*, Vol. 2, 1965, pp. 561–565.
11. A. Singh and J. K. Mitchell, 'General stress-strain-time function for soils', *J. Soil Mech.* ASCE, **94,** 31–46 (1968).
12. A. K. Parkin, 'Creep of rockfill', *Advances in Rockfill Structures*, Kluwer Academic Publishers, Boston, 1991, pp. 221–238.
13. J. L. Justo, *Deformación de las Presas de Escollera*, Fundación Juan March, Madrid 1968.
14. R. J. Marsal, E. Moreno, A. Núñez, R. Cuéllar and R. Moreno, '*Research on the Behaviour of Granular Materials and Rockfill Samples*', Comisión Federal de Electricidad, México, DF, 1965.

15. W. G. Holtz and J. W. Hilf, 'Settlement of soil foundations due to saturation', *Proc. 5th Int. Conf. Soil Mech. FE.*, Vol. 1, 1961, pp. 673–679.
16. N. L. de S. Pinto, P. L. Marques and E. Filho, 'Foz the Areia Dam-Design, Construction and Behaviour', *Concrete Face Rockfill Dams-Design, Construction and Performance*. ASCE, 1985, pp. 173–207.
17. A. S. Vesic and G. W. Clough, 'Behaviour of granular materials under high stresses', *J. Soil Mech.*, ASCE, **94,** 661–688 (1968).
18. N. O. Boughton, 'Elastic analysis for behaviour of rockfill', *J. Soil Mech.* ASCE, **96** (SM5), 1715–1733 (1970).
19. R. E. Gibson and K. Y. Lo, 'A theory of consolidation for soils exhibiting secondary compression', Publication No. 41, NGI, 1961.
20. I. F. Christie, 'A re-appraisal of Merchant's contribution to the theory of consolidation', *Geotechnique*, **14,** 309–320 (1964).
21. W. J. Thompson, 'Some deformation characteristics of a saturated remoulded silty clay', *Proc. 6th Int. Conf. Soil Mech. & F.E.*, Vol. 1, 1965, pp. 373–376.
22. O. C. Zienkiewicz, M. Watson and I. P. King, 'A numerical method of visco-elastic stress analysis', *Int. J. Mech. Sci.* Pergamon, **10,** 807–827 (1968).
23. J. A. Charles, 'The use of one-dimensional compression tests and elastic theory in predicting deformations of rockfill embankments', *Can. Geotech. J.*, **13,** 189–200 (1976).
24. J. L. Justo, P. Cañete, J. L. Manzanares, J. Del Campo and P. De Porcellinis, 'The upstream facing of Martin Gonzalo rockfill dam', *Trans. 16th Int. Cong. on Large Dams*, Vol. 2, San Francisco, 1988, pp. 815–837.
25. D. J. Naylor, J. R. Maranha, E. Maranha das Neves and A. A. Veiga Pinto, 'A back-analysis of Beliche Dam', *Géotechnique*, **47,** 221–233 (1998).
26. J. H. Dudley, 'Review of collapsing soils', *J. Soil Mech.* ASCE, **96,** 925–947 (1970).
27. E. S. Nobari and J. M. Duncan, *Effect of Reservoir Filling on Stresses and Movements in Earth and Rockfill Dams*, U.S. Army Waterways Experiment Station, Contract report 5-72-2, 1972.
28. K. Terzaghi, 'Discussions', Trans. ASCE, **125**(2A)**,** 139–148.
29. J. A. Jiménez Salas and J. L. Justo, 'General Report: Engineering geological aspects of foundations in soils' *Proc. 5th Int. Cong. Int. Ass. Engineering Geology*, Buenos Aires, Vol. 8, 1986, pp. 2519–2598.
30. A. Josa, Un modelo elastoplástico para Suelos no Saturados, *Ph.D. Thesis*, Politechnical University of Cataluña, Barcelona, Spain, 1988.
31. B. Materon, 'Alto Anchicaya dam-ten years performance', *Concrete Face Rockfill Dams-Design, Construction and Performance*. ASCE, 1985, pp. 73–87.
32. Y. C. Fung, *Foundations of Solid Mechanics*, Prentice-Hall, Englewood Cliffs, NJ, 1965.
33. J. L. Justo, 'The failure of the impervious facing of Martin Gonzalo rockfill dam', *Trans. 16th Int. Cong. On Large Dams*, Vol. 5, San Francisco, Expert Report, pp. 252–262.
34. J. L. Justo, F. Segovia and A. Jaramillo, 'La utilización de rocas de baja resistencia en los pedraplenes de rocas de materiales sueltos', *Simp. sobre Terraplenes, Pedraplenes y otros Rellenos*, Madrid, Soc. Esp. Mec. Suelo, pp. 446–479.
35. S. Lemercier, *Etude des barrages en remblais*', Projet de recherche, E.T.S. Arquitectura, University of Seville, 1996.

